ACS OMEGA

http://pubs.acs.org/journal/acsodf

Article

Graphene Oxide-Functionalized Thread-Based Electrofluidic Approach for DNA Hybridization

Liang Wu, Arushi Manchanda, Vipul Gupta, and Brett Paull*

Cite This: *ACS Omega* 2023, 8, 13569−13577

Read Online

ACCESS | Metrics & More | Article Recommendations | Supporting Information

ABSTRACT: A novel, low-cost, and disposable thread-based electrofluidic analytical method employing isotachophoresis (ITP) was developed for demonstrating surface DNA hybridization. This approach was based on graphene oxide (GO) surface-functionalized zones on nylon threads as a binding platform to trap a fluorescently labeled isotachophoretically focused single-stranded DNA (ssDNA) band, resulting in quenching of the fluorescence, which signaled quantitative trapping. In the event of an isotachophoretically focused complementary DNA (cDNA) band passing over the GO-trapped ssDNA zone, surface hybridization of the ssDNA and cDNA to form double-stranded DNA (dsDNA) band occurred, which is released from the GO-coated zones, resulting in restoration of the fluorescent signal as it exits the GO band and migrates further along the thread. This controllable process demonstrates the potential of the GO-functionalized thread-based microfluidic analytical approach for DNA hybridization and its visualization, which could be adapted into point-of-care (POC) diagnostic devices for real-world applications.

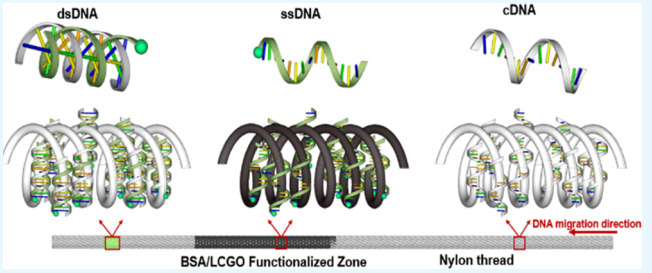

1. INTRODUCTION

DNA hybridization[1] involves the formation of a double-stranded nucleic acid (either a DNA double helix or an RNA−DNA duplex) from two complementary single strands and can be applied within diagnostic and bioanalytical workflows,[2,3] based upon the ability of a single strand to specifically and selectively identify its complementary target strand, at low concentration, among a large population of unrelated DNA sequences.[4] Applications of DNA hybridization include the determination of relatedness between species, detection of single-base mutations, diagnosis of genetic diseases, DNA sequencing, and DNA synthesis.[4,5] However, controlled DNA hybridization within simple microfluidic and microarray-based platforms is nontrivial, and issues such as slow diffusion, uncontrolled transport, and slow reaction rates often hinder practical performance at low concentrations. Despite this, simple, sensitive, highly selective, and cost-effective point-of-care (POC) diagnostic platforms aimed at addressing global health issues (such as infectious diseases), based upon standalone microfluidics[6,7] or microfluidics in combination with microarrays,[8] each exploiting the selectivity of DNA hybridization, have been successfully developed.[9−12] For example, Song's group reported a microfluidic concentration device, with a maximum concentration factor of ∼800, aimed at accelerating the surface hybridization reaction between DNA and morpholinos to within 15 min, which could be applied with a concentrator-enhanced microarray detection system for diagnostic assays.[13]

Microfluidic thread-based analytical devices (μTADs), which utilize threads to construct fluidic channels to perform various analytical assays,[14,15] show great potential to deliver POC diagnostics within resource-limited situations, principally due to low-cost, simplicity, biocompatibility, low reagent consumption, and mechanical strength when wet.[16] Where electric fields are applied to control or manipulate the flow of liquids across and through the threads, the term "electrofluidic thread-based analytical devices" (eTADs) can be used to distinguish between approaches.[17] Various applications of μTAD/eTADs have recently been reported across a variety of areas, including cell culture analysis,[18] electrochemical detection systems,[19] DNA focusing,[20] metabolite analysis,[17] and antibody detection.[21] Thread-based systems are also readily compatible with both optical and electrochemical detection methods, which is significant as both fluorescent and electrochemical tags are commonly used to enhance the sensitivity and detection of DNA.[22,23]

A further advantage of the use of threads is the ease of surface modification and, in particular, the ease of functionalization using nanomaterials. For example, graphene oxide (GO) (the water−soluble derivative of graphene[24]) has been used to functionalize the surface of threads and yarns (e.g., nylon, cotton, polyester, and even pyroprotein-based fibers[25])

Received: September 26, 2022
Accepted: March 28, 2023
Published: April 3, 2023

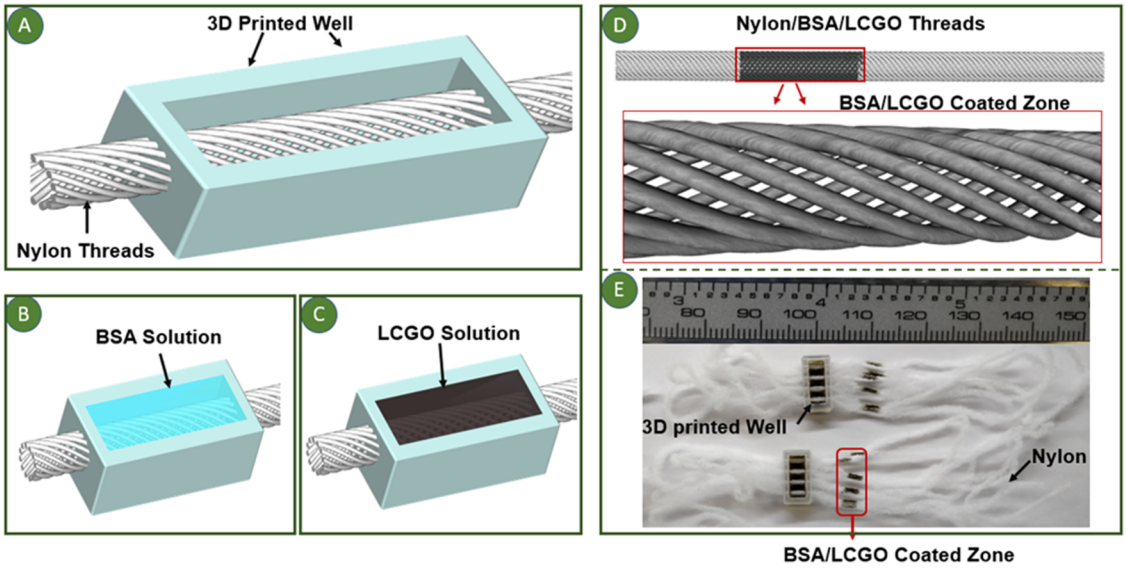

Figure 1. Fabrication of BSA/LCGO-coated nylon threads. (A) Thread in a 3D-printed well; (B) BSA surface functionalization on nylon thread; (C) LCGO surface functionalization on BSA-coated nylon threads; (D) schematic image of a BSA/LCGO-coated zone on nylon thread; and (E) optical image of BSA/LCGO-coated zone (3 mm in length) on nylon threads.

to form flexible and durable graphene-based electronic textiles.[26] More importantly, GO has been successfully used to interact with DNA molecules,[27−32] including for DNA hybridization, exploiting three very advantageous properties.[21] Firstly, GO, with an extremely large surface area-to-volume ratio, provides significant capacity for the interaction and retention of biomolecules. Secondly, GO exhibits markedly different selectivity toward single-stranded DNA (ssDNA) over double-stranded DNA (dsDNA). Thirdly, GO can be used as a simple self-indicator of DNA adsorption, as it is a universal fluorescence quencher[29] for most fluorescent tags and quantum dots.[33]

Isotachophoresis (ITP) is an electrophoretic separation method typically carried out within capillaries. However, the technique has gained increasing application in the area of DNA analysis over recent years.[34,35] Up to 14 000-fold increases in DNA hybridization rates have been reported using ITP.[36] Further, when compared to conventional methods,[34] ITP-enhanced microarrays were reported to provide hybridization at a much faster rate (30 min versus 20 h) and with higher sensitivity (∼8.2-fold). Recently, we applied ITP to isolate and preconcentrate DNA from biological samples using a simple eTAD prior to off-thread polymerase chain reaction (PCR) analysis.[20]

In the work presented herein, an electrofluidic thread-based method, applying ITP and incorporating a nylon thread with a GO-coated DNA concentration zone, is demonstrated for controlled DNA hybridization. A dye-labeled ssDNA was used as a probe to investigate the absorption and desorption of DNA from the GO-coated zone. ITP was used to preconcentrate and deliver the complementary DNA into the functionalized zone and facilitate the rapid and selective hybridization of DNA and its subsequent controlled migration from the GO-coated region. To the best of our knowledge, to date, GO surface-functionalized threads, together with a controlled on-fiber ITP electrofluidic approach, have not been combined previously to facilitate and confirm DNA hybridization in such a rapid, selective, and controlled manner.

2. EXPERIMENTAL SECTION

2.1. Reagents and Materials. *2.1.1. Buffer Solution Preparation.* Tris-(hydroxyl methyl) amino-methane (TRIS), 4-(2-hydroxyethyl)-1-piperazineethanesulfonic acid (HEPES), hydrochloric acid, and poly(vinylpyrrolidone) (PVP) were obtained from Sigma-Aldrich (New South Wales, Australia). Solutions were prepared in water sourced from a Milli-Q Water Plus system by Millipore (Bedford, Massachusetts).

2.1.2. DNA Solution Preparation. 29.8 nmol of ssDNA (a Homo sapiens tumor suppressor gene (exon segments of p53 gene) with sequence 5′-FAM (fluorescein amidite)-CTGTCTTGAACATGAGTT-3′), 16.7 nmol of cDNA (5′-AACTCATGTTCAAGACAG-3′), and a reconstitution solution (10 mM Tris-HCl (pH 8.0), 0.1 mM EDTA, 50 mL) were purchased from Thermo Scientific (Victoria, Australia). 0.05−5.0 μM ssDNA and cDNA solutions were prepared in this study.

2.1.3. Nylon Thread Preparation. 100% nylon bundle thread (diameter (Ø) of 500 μm, woolly nylon stretches overlocking thread, QA Thread, China) was used. Nylon was chosen here as it has been demonstrated to exhibit negligible surface adsorption of DNA.[20] The threads were sequentially washed using Milli-Q water and methanol (100%) in an ultrasonic bath for 10 min, which was repeated three times to remove impurities from the surface. Subsequently, the threads were dried at room temperature before they were plasma-treated for 2 min at 18 W by a vacuum plasma reactor (K1050X plasma asher (Quorum Emitech, U.K.)) to increase the wetting and wicking properties of the thread.[14,37]

2.1.4. Bovine Serum Albumin (BSA) Solution Preparation. The BSA powder (Sigma-Aldrich NSW, Australia) was diluted to the desired concentration (0.5 wt %) in Milli-Q water and filtered through a 0.22 μm Millipore filter. The BSA solutions were freshly prepared for each experiment or were otherwise stored at 2−4 °C to reduce protein aggregation.

2.1.5. Synthesis of Liquid Crystalline Graphene Oxide (LCGO). Based on a previously described GO synthesis protocol,[38] LCGO was prepared from natural graphite flakes using a chemical method with H_2SO_4, HNO_3, H_2O_2, and

https://doi.org/10.1021/acsomega.2c06228
ACS Omega 2023, 8, 13569−13577

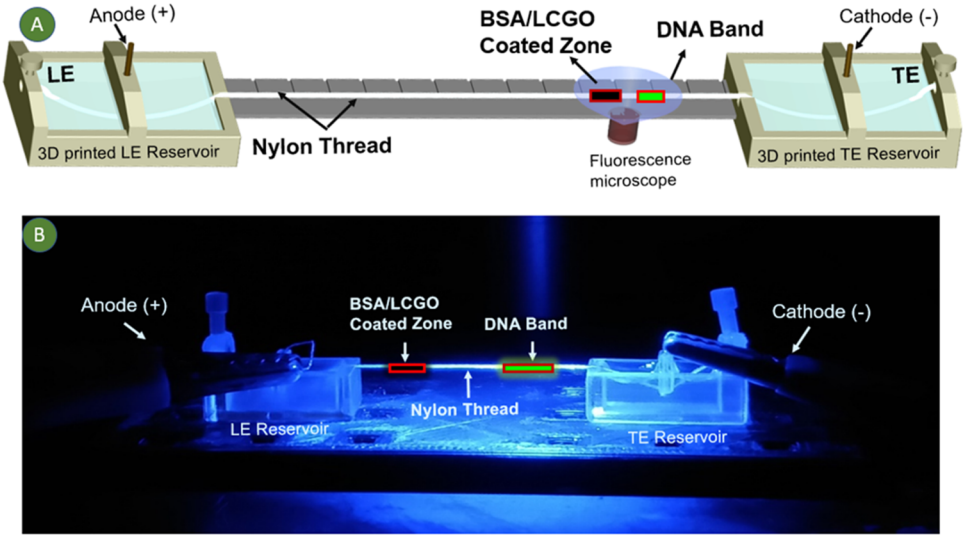

Figure 2. Electrofluidic BSA/LCGO/nylon thread-based analytical device. (A) Schematic presentation of LCGO-coated eTAD. (B) Experimental presentation of LCGO-coated eTAD setup. TE: terminating electrolyte and LE: leading electrolyte.

$KMnO_4$. Suspensions of ultra-large LCGO sheets with a lateral size of up to ca. 100 μm were produced[39] and provided by researchers at the University of Wollongong, Australia. LCGO, with a high aspect ratio of over 30 000,[38] was used here due to its self-assembled brick-like nanostructures and a high degree of orientation, which had the capability to reproducibly form a full homogeneous functional coating upon the threads.

2.2. BSA/LCGO-Coated Nylon Threads. BSA/LCGO-coated nylon threads were prepared in the following manner. First, the plasma-treated nylon threads were drawn through a three-dimensional (3D) printed well (inner chamber dimensions: 1−3 mm width × 8 mm length × 2 mm height, see Figure 1A) via two holes (300 μm in diameter), produced using an Eden 260VS 3D printer (Stratasys, Minnesota), with VeroClear as the build material and SUP707 as the support material. The holes were designed to constrict the threads and limit the leakage of solution via the wicking property of the threads. For BSA functionalization, a 0.5 wt % BSA solution of 16−48 μL was then added into the well to fully cover the immobilized threads, see Figure 1B (also shown in Supporting Information Video 1). The BSA-coated nylon threads were then dried in situ within a fume hood for 30 min. BSA is able to strongly adsorb to both organic and inorganic materials, including nylon, through hydrophobic (nonpolar) and hydrophilic (polar) interactions,[40] and has been shown previously as a universal adhesive for improving the adsorption of LCGO onto various surfaces.[26] Next, a 1−3 mg mL^{-1} GO solution (pH = 3.0−4.0) of 16−48 μL was pipetted into the well to cover the BSA-coated nylon threads, with mild agitation to enable the self-assembly of the GO nanosheets upon all of the surfaces of the BSA-coated nylon, see Figure 1C (also shown in Supporting Information Video 1). The LCGO/BSA-modified nylon threads were then again dried in situ in a fume hood for 30 min before these threads were removed from the well. The LCGO/BSA-coated regions (Figure 1D) on the threads were clearly restricted to within the designed dimensions using this new approach (see Supporting Information Table S1 and Figures S1 and 1E), as opposed to less precise modification methods reported previously.[41] This modification technique also provides a means for additional functionalization of precise zones of the threads for their future use in simple and cost-effective POC diagnostic platforms.

2.3. Electrofluidic Thread-Based Analytical Devices (eTADs). The eTAD shown in Figure 2A consists of a rectangular 3D-printed polylactic acid (PLA) base, two platinum wires (30 μm in diameter) as electrodes, nylon threads, and inlet- and outlet buffer reservoirs. The base (120 mm length × 80 mm width × 50 mm height) with two 3 mm square holes (located on the left and right side of the base) was accurately designed using SolidWorks CAD software (SolidWorks Corp., Dassault Systemes, France) and was prepared using a commercial desktop FELIX 3D FDM printer (Nieuwegein, the Netherlands), to provide positions for the installation of the buffer reservoirs. The buffer reservoirs holding terminating electrolyte (TE) and leading electrolyte (LE) buffers (Figure 2B) were also designed using SolidWorks and printed using an Eden 260VS 3D printer (Stratasys, Minnesota) with VeroClear as the build material and SUP707 as the support material. In accordance with our previous work,[17,20] assembly of the eTAD involved a two-stage process (Figure 2). First, the buffer reservoirs were inserted into the square holes of the PLA base to allow easy adjustment to the desired thread length (32 mm). Second, the thread was tightened via screws across to the holders of each buffer reservoir. In all experiments, the threads were kept wet with buffer solutions (LE) during the separation process.

2.4. Thread-Based (TB) Isotachophoresis (ITP) Operation. 5 mM TRIS/2.5 mM HEPES (pH 8.54) was used as the terminating electrolyte (TE) solution, and 20 mM TRIS/10 mM HCl (pH 8.53) as the leading electrolyte (LE) solution for all ITP experiments. 0.1 wt % PVP was added into the LE and TE solutions to eliminate the electroosmotic flow. The nylon thread was loaded into the eTAD after it was presoaked with the LE solution. The BSA/LCGO-coated zone was located at a distance of 1 cm from the LE buffer reservoir for the trapping of ITP focused DNA. Platinum (Pt) wires were inserted into the capillary holes in the middle of each reservoir to serve as polarizing electrodes. TE and LE buffers of 500 μL were added into the TE (left chamber) and the LE reservoir (right chamber), respectively. The TB-ITP experiments were performed in positive mode with the anode in the inlet and the

https://doi.org/10.1021/acsomega.2c06228
ACS Omega 2023, 8, 13569−13577

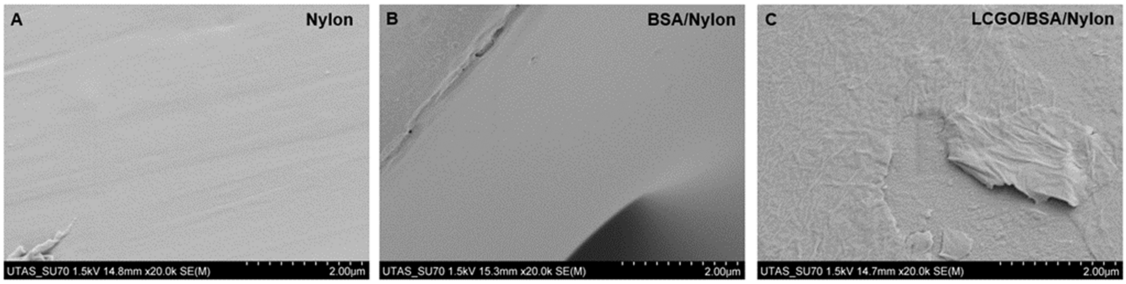

Figure 3. SEM images of BSA/LCGO/nylon threads. (A) Uncoated nylon; (B) BSA-coated nylon; and (C) LCGO/BSA-coated nylon (1 mg mL^{-1}).

cathode in the outlet buffer reservoir. Voltage or current was applied using an in-house built 4-channel (0−5 kV) DC power supply interfaced to a computer using a 12-Bit, 10 kS s^{-1} multifunction DAQ system (USB-6008 OEM, National Instruments, Austin, Texas). Before applying any voltage or current, the thread was wetted with 5 μL of the LE buffer and then allowed to equilibrate for 1 min, reducing any capillary action along the thread. Then, a 1 μL drop (by micro-pipette) of 5.0 μM DNA solution (either ssDNA, cDNA, or dsDNA) was applied directly onto the threads at 1.0 ± 0.1 cm from the inlet reservoir. A constant current of 100 μA was applied to initiate the ITP procedure, as low current reduces the generation of Joule heating.[42] Joule heating is problematic as it can cause unwanted effects, such as water evaporation, burnout of the thread itself, reduction of DNA fluorescence due to reduced quantum yield of the fluorophore,[30] and inhibition of DNA hybridization. A USB microscope AM4113T-GFBW (Dino-Lite Premier, Clarkson, WA, Australia) equipped with a blue light-emitting diode for excitation and a 510 nm emission filter was used to record the migration along the thread and continuous focusing of the fluorescently labeled DNA between the TE and LE. Fluorescence intensities of images and videos were processed with ImageJ software, analyzing the region of interest (ROI) and then monitoring the mean fluorescence intensity value of the ROI versus time.

The composition of the fluorescent band eluted from graphene after the hybridization experiment was examined using a capillary electrophoresis-based fragment analyzer (5200 fragment analyzer, Agilent Technologies, California). In these experiments, 5.0 μM × 1 μL ssDNA and 5.0 μM × 1 μL cDNA were employed to carry out the hybridization experiments. The eluted band was extracted from the thread by simply cutting out the section of the thread where the band was focused and extracting its contents in an Eppendorf tube, as described in our previous report.[20] Briefly, the collected section of the thread was introduced into an empty 0.5 mL Eppendorf tube, which was previously impaled such that only the contents of the threads could be transferred out of it and not the actual thread during centrifugation. The impaled tube was placed in a receiving Eppendorf tube (2 mL) and centrifuged at 2000 rpm for 5 min, where all of the contents were collected in the receiving tube and analyzed with the fragment analyzer as is. Any additional solvent was not used for extraction to minimize any sample dilution. 2 μL of the extracted sample was analyzed via a fragment analyzer.

3. RESULTS AND DISCUSSION

3.1. Preparation and Characterization of BSA/LCGO/Nylon Threads. The BSA/LCGO/nylon threads were fabricated in two consecutive steps: (i) threads were functionalized with BSA molecules which introduced positive charges on the surface of the nylon, (ii) a LCGO nanosheet coating with negative charges was formed on the BSA-functionalized nylon via electrostatic self-assembly.[26] Some color variations on the BSA/LCGO-coated areas were observed, which was presumably due to variations in the thickness of LCGO coating on the threads. In order to investigate the homogeneity of the LCGO coating on the threads, particularly for the areas with relatively bright colors, the morphology of these functionalized zones was examined using scanning electron microscopy (SEM), shown in Figure 3. From Figure 3, it can be seen that the impact of BSA on the surface of nylon was visibly negligible (Figure 3B); however, wrinkles, ripples, and even layer-like structures were clearly observed on the surfaces of LCGO/BSA-coated nylon (Figure 3C). This was likely due to the wrapping of the LCGO nanosheets, confirming strong electrostatic interaction between the positively charged BSA-coated nylon and the negatively charged LCGO sheets.

3.2. eTADs-ITP for DNA Hybridization. A BSA/LCGO/nylon thread was used within an eTAD, employing an ITP-based process for controlled DNA hybridization. The procedure was composed of two main operations. The first was ssDNA migration, focusing, and selective absorption on GO at the BSA/LCGO-coated zone (Supporting Information Video 2). The second was ssDNA desorption from GO via on-surface hybridization with focused cDNA to form unretained dsDNA (Supporting Information Video 3). Figure 4 shows schematic and fluorescent images of the FAM-labeled ssDNA adsorption process and its subsequent desorption as dsDNA from the BSA/LCGO/nylon threads. In these experiments, 5.0 μM × 1 μL ssDNA, 5.0 μM × 1 μL cDNA, and LCGO/BSA-coated (3 mm zone, loaded with 3 mg mL^{-1} LCGO solution) nylon threads were employed to carry out the hybridization experiments shown (see Supporting Information Table S2). Figure 4A shows a fluorescent and schematic image of a nylon thread with a BSA/LCGO-coated zone. Figure 4B shows a highly fluorescent ITP focused ssDNA (FAM-tagged) band, which was clearly observed on the thread. The bandwidth of the sample plug remained constant while the applied field was maintained. The mobility of the negatively charged ssDNA was greater than HEPES (HEPES mobility: 23.50 $cm^2\ V^{-1}\ s^{-1}$) and less than Cl^- (Cl^- mobility: 79.10 $cm^2\ V^{-1}\ s^{-1}$), which caused the ssDNA to stack at the boundary between the TE and the LE.[20]

Figure 4C−E illustrates how a highly fluorescent focused ssDNA band migrates into the BSA/LCGO-coated zone, with immediate quenching of the majority of fluorescence and the subsequent emergence from the outlet side of the GO trap of a

https://doi.org/10.1021/acsomega.2c06228
ACS Omega 2023, 8, 13569−13577

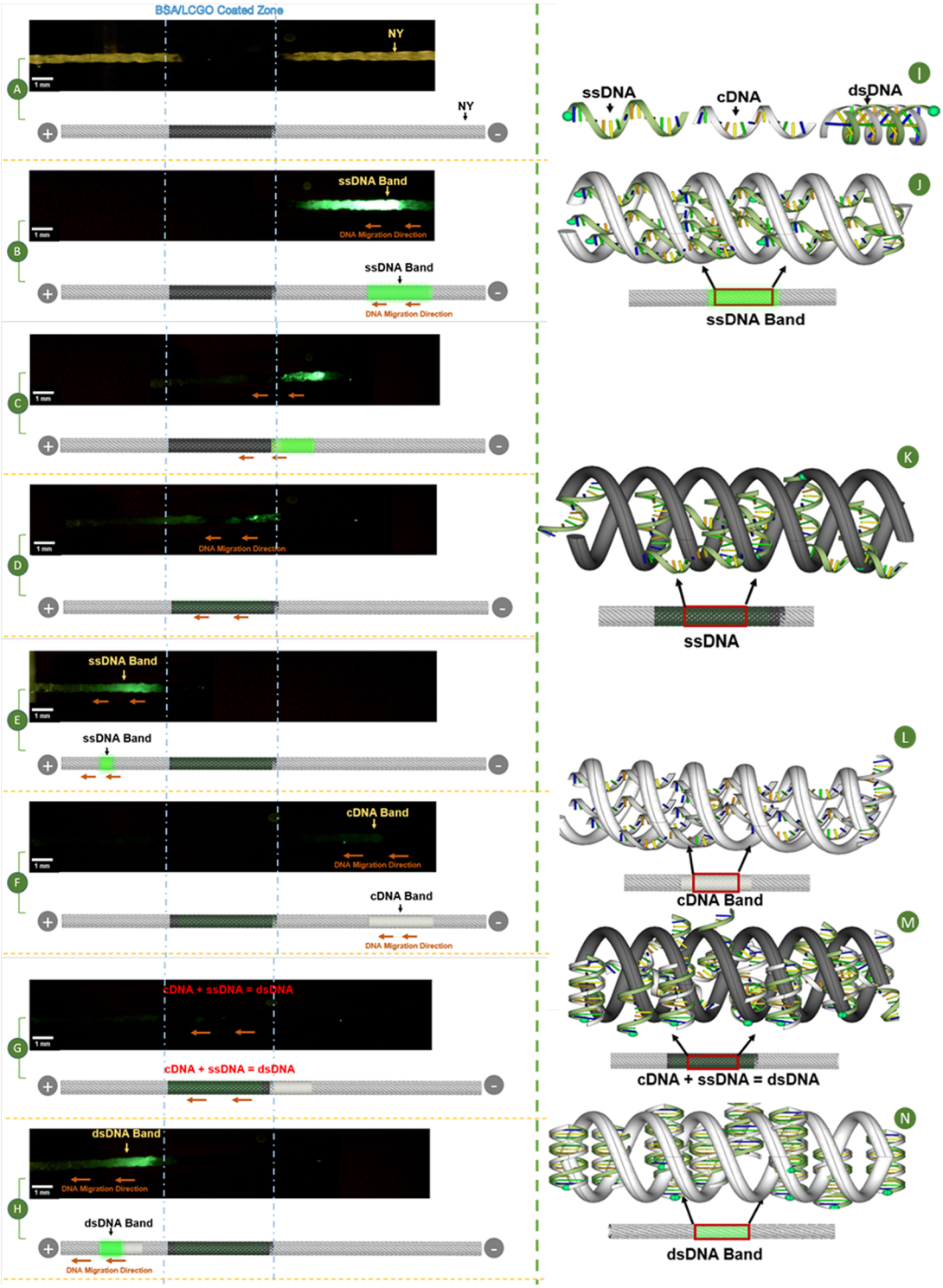

Figure 4. Shows BSA/LCGO/nylon thread-based ITP approach for DNA hybridization. (A) Fluorescent and schematic image of a nylon thread with a BSA/LCGO-coated zone. (B) Fluorescent and schematic image of a highly focused FAM-tagged ssDNA band on the nylon thread. (C) Fluorescent and schematic image of the ssDNA band migrating to the BSA/LCGO-coated zone. (D) Fluorescent and schematic image of the ssDNA band on the coated zone. (E) Fluorescent and schematic image of a narrow ssDNA band passing through the coated zone and migrating to LE reservoir. (F) Fluorescent and schematic image of a cDNA band on the nylon thread. (G) Fluorescent and schematic image of the cDNA band migrated to the coated zone where ssDNA was trapped. (H) Fluorescent and schematic image of a dsDNA band on nylon thread migrating to LE reservoir. (I) Schematic representation of ssDNA, cDNA, and dsDNA. (J) Schematic representation of an isotachophoretically focused ssDNA band on the nylon. (K) Schematic representation of an isotachophoretically focused ssDNA band on the LCGO/BSA-coated zone of the nylon. (L) Schematic representation of an isotachophoretically focused cDNA band on the nylon. (M) Schematic representation of an isotachophoretically focused ssDNA and cDNA band complexation on the LCGO/BSA-coated zone of the nylon. (N) Schematic representation of an isotachophoretically focused dsDNA band on the nylon.

https://doi.org/10.1021/acsomega.2c06228
ACS Omega 2023, 8, 13569−13577

low-intensity fluorescent band of unretained ssDNA. This is also shown in Supporting Information Video 2. The migration of the band was clearly observed, starting from the right of the coated zone (shown in Figure 4C), then through the whole zone (shown in Figure 4D), and ending up on the left (Figure 4E). It took approximately 5 min to complete the migration procedure. As noted above, the fluorescence of ssDNA was primarily quenched by the BSA/LCGO-coated zone upon adsorption, even though both the GO and the ssDNA were negatively charged. This is because the ssDNA is selectively immobilized on the surface of GO layers through $\pi-\pi$ interactions between G or GO and the aromatic bases.[29,43] In addition to DNA base stacking with the hydrophobic domains, hydrogen bonding and electrostatic repulsion with the oxygen-rich domains are also likely to occur.[44]

Figure 4F−H shows a process under which a nontagged cDNA band was loaded, focused, and driven to migrate into the coated zone. A very weak fluorescence band (Figure 4F) was gradually observed during the migration due to the interaction between cDNA and the remaining ssDNA on the thread. However, Figure 4H then shows a strongly fluorescent band clearly reappearing at the left of the coated zone, and the band was further driven to migrate into the LE reservoir. This band represents the now fluorescently tagged dsDNA formed via surface hybridization on the GO trap (see Supporting Information Video 3). Upon forming dsDNA, the DNA bases are hidden within the helical structure and no longer available for surface binding, resulting in release from the GO trap due to the disruption of hydrophobic interactions. Only the negatively charged phosphate groups remain exposed.[29,30] Therefore, after the ssDNA hybridizes with its cDNA to form dsDNA, the FAM fluorescence of ssDNA remains.

To verify that the migrating fluorescently labeled band exiting the GO was indeed majoritively dsDNA, the migrating band was cut from the thread, extracted from the thread, and analyzed using a capillary electrophoresis-based fragment analyzer (as described in Section 2.4 above). The results of this confirmatory analysis (see Supporting Information Figure S2) on the extracted fluorescent band showed the presence of 60% dsDNA and 20% of each ssDNA and cDNA, thereby confirming hybridization.

It was also observed that there was a clear fluorescent intensity difference before and after the ssDNA band migrated through the GO-coated zone. Figure 5A shows the intensity differences of the ssDNA band with and without adsorption onto GO. The quenching kinetics were fairly fast, with the vast majority of fluorescence quenching taking place. Figure 5B also suggests that the fluorescence quenching within the coated zone is directly related to the amount of ssDNA adsorbed. When the amount of ssDNA (such as 5 μM × 1 μL) was more than the absorption capacity of the coated zone, the extra ssDNA continued to migrate to the inlet reservoir after passing through the zone (shown in Supporting Information Video 2) in this case. When the amount of ssDNA (such as 0.05 μM × 1 μL) was less than the capacity of the coated zone, the ssDNA was fully adsorbed and quenched, which is shown in Supporting Information Video 4. However, when the amount of ssDNA is significantly less than the capacity of the coated zone, both ssDNA and cDNA would be trapped, which compromises the formation of dsDNA and then reduces the fluorescent detection efficiency. The two parameters (the amount of DNA and the capacity of the LCGO-coated zone) therefore can be used when it comes to optimizing the desired

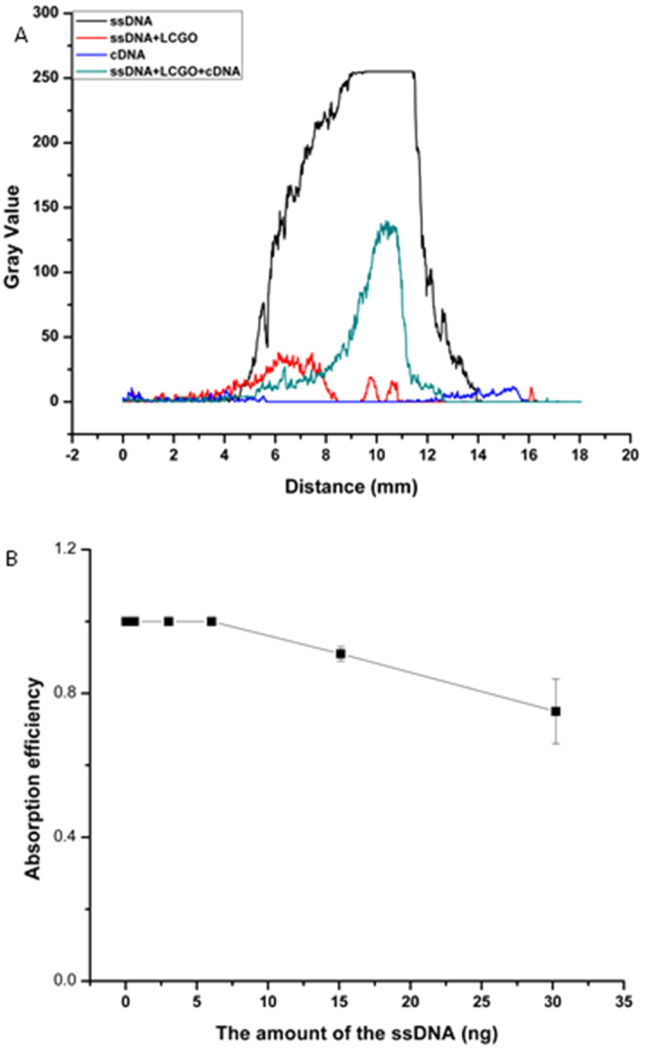

Figure 5. (A) Fluorescent intensity (represented by gray value) of ssDNA on (red) and off (black) the LCGO/BSA-coated zone. The fluorescent intensity of dsDNA (olive) after the desorption of ssDNA from the LCGO/BSA-coated zone due to complexing with cDNA (blue). (B) Absorption efficiency of 3 mg mL^{-1}−3 mm LCGO/BSA-coated zone vs the amount of the loaded ssDNA.

design and sensing performance for eTADs under development. For example, 1 mg mL^{-1} loaded—1 mm length LCGO/BSA-coated nylon would be suitable to investigate the DNA hybridization microarrays at low concentrations (such as 0.01 μM), while 3 mg mL^{-1} loaded—3 mm length LCGO/BSA-coated nylon can be adapted for hybridizing DNA at higher concentration (such as 5 μM).

In addition, it should be noted that the fluorescence of ssDNA before adsorption was more intensive than after desorption (see Figure 5A). This indicates that a certain amount of the ssDNA was still adsorbed or trapped by the GO within the coated zone. To further investigate whether the desorption of ssDNA was fully completed, cDNA was repeatedly added onto the thread. Figure 6 shows that desorption of the ssDNA (as dsDNA) remained evident even after the cDNA was loaded three times, from the observation of the fluorescence band. The intensity and width of the fluorescent band reduced gradually with multiple loads of cDNA. This suggests that ssDNA that was previously trapped by the GO was gradually released as a part of the

https://doi.org/10.1021/acsomega.2c06228
ACS Omega 2023, 8, 13569−13577

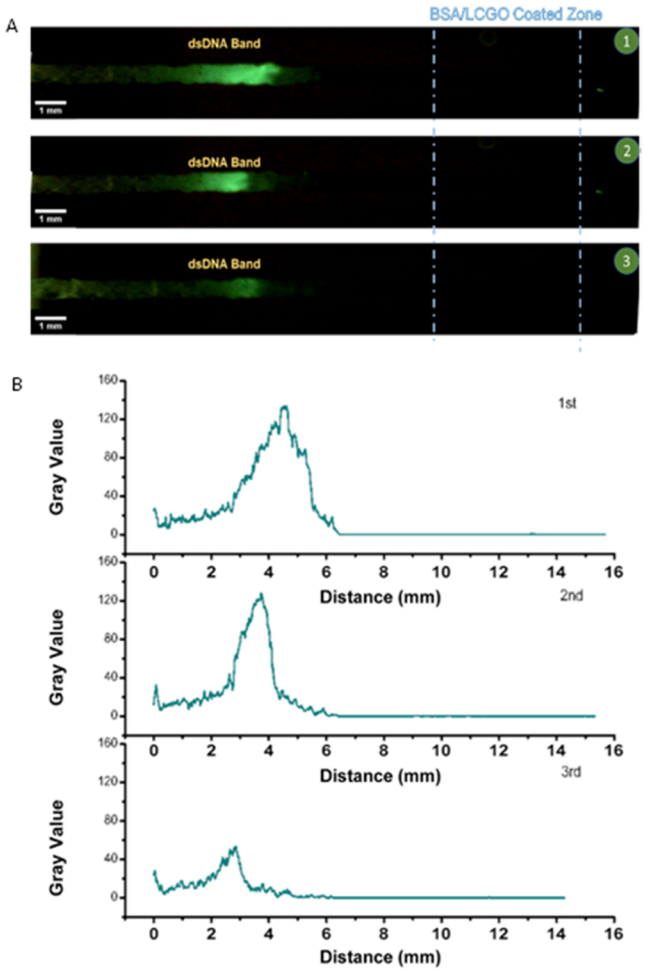

Figure 6. (A) Fluorescent images of the desorption of ssDNA (as dsDNA) with three sequential loads of cDNA. (B) Fluorescent intensity of dsDNA after the desorption of ssDNA from the LCGO/BSA-coated zone with three sequential loads of cDNA (Supporting Information Table 2 shows more information about the steps of the DNA hybridization procedure).

formed dsDNA. This observation may help to optimize GO-based thread approaches for DNA detection and analysis for future applications.

Furthermore, compared to ssDNA, GO has a low sorption affinity toward dsDNA.[30] This means that the binding between dsDNA and GO is weak, and dsDNA is more likely to migrate through the coated zone. In order to investigate the interaction between dsDNA and GO, 1 μL of dsDNA (formed by mixing 5.0 μM ssDNA with 5.0 μM cDNA at room temperature) was employed under the same experimental conditions as ssDNA. The fluorescence intensity of the dsDNA band exhibited a relatively small change before and after migrating through the coated zone (see Supporting Information Video 5). This demonstrates that the dsDNA migrated through the coated zone without being obviously trapped. This further indicates that the migration of dsDNA would occur quickly through the coated zone once it is formed from hybridization.

4. FURTHER DISCUSSION

In this study, a novel LCGO-coated nylon thread-based electrofluidic approach was demonstrated for DNA hybridization using ITP. At this proof of principle development stage, the results were very promising, which leaves scope for optimization and developments toward possible applications. First of all, as this approach is at its initial development state, potential improvements for further work would aim to investigate the interaction between ssDNA and its mismatched DNA (such as single-base mismatched and completely mismatched sequences) to further demonstrate its selectivity. Also, it would be worth investigating whether other effects (such as the number of DNA bases and the kinetics of the DNA adsorption/desorption[30]) would affect the procedure of DNA hybridization (such as the hybridization time, hybridization specificity, and sensitivity). For potential applications, the approach demonstrated here presents a potential strategy for the development of flexible biosensors for POC diagnostics and health state monitoring.[45,46] Furthermore, LCGO-coated biocompatible threads provide more possibilities to be integrated into smart wearable systems (SWSs) and implantable diagnostic devices (IDDs) that are capable of in situ sample collection for diagnosing and treating diseases.[47] As reduced LCGO-coated threads can also be electrically conductive, significant opportunities to develop bipolar electrode zones for bipolar electrochemical analysis of DNA are also possible.[48]

5. CONCLUSIONS

A simple and feasible method to fabricate sectionally surface-functionalized nylon threads using LCGO was demonstrated. LCGO/nylon threads were obtained from LCGO wrapping with BSA via electrostatic self-assembly. BSA served as a universal adhesive to improve the GO sheets wrapping onto the nylon. LCGO/BSA/nylon threads were then integrated into the eTAD for DNA hybridization through the electrofluidic assay due to the selective interactions between the ssDNA and dsDNA and the GO. Furthermore, ITP was employed on these functional threads to preconcentrate DNA to increase the speed and sensitivity of the on-thread DNA hybridization. It was demonstrated that the LCGO/BSA-coated zone produced significant fluorescence quenching as well as great sorption affinity toward ssDNA. cDNA played a key role in the desorption of ssDNA from functional regions after complexing with ssDNA to form dsDNA. The approach demonstrated here provides a simple and potentially high-throughput analysis method for rapid and selective DNA hybridization and screening.

■ ASSOCIATED CONTENT

Supporting Information

The Supporting Information is available free of charge at https://pubs.acs.org/doi/10.1021/acsomega.2c06228.

Preparation conditions of BSA/LCGO/Nylon threads (PDF)

LCGO/BSA/Nylon threads with 1, 2, and 3 mm in length (MP4)

SEM images of BSA/LCGO/nylon threads (MP4)

DNA hybridization procedure on LCGO/BSA/nylon threads (MP4)

Results of capillary electrophoresis-based fragment analyzer (MP4)

https://doi.org/10.1021/acsomega.2c06228
ACS Omega 2023, 8, 13569−13577

AUTHOR INFORMATION

Corresponding Author

Brett Paull − *Australian Centre for Research on Separation Science (ACROSS) and ARC Centre of Excellence for Electromaterials Science (ACES), School of Natural Sciences (Chemistry), University of Tasmania, Hobart 7001 Tasmania, Australia;* orcid.org/0000-0001-6373-6582; Email: brett.paull@utas.edu.au

Authors

Liang Wu − *Australian Centre for Research on Separation Science (ACROSS) and ARC Centre of Excellence for Electromaterials Science (ACES), School of Natural Sciences (Chemistry), University of Tasmania, Hobart 7001 Tasmania, Australia*

Arushi Manchanda − *Australian Centre for Research on Separation Science (ACROSS) and ARC Centre of Excellence for Electromaterials Science (ACES), School of Natural Sciences (Chemistry), University of Tasmania, Hobart 7001 Tasmania, Australia*

Vipul Gupta − *Australian Centre for Research on Separation Science (ACROSS) and ARC Centre of Excellence for Electromaterials Science (ACES), School of Natural Sciences (Chemistry), University of Tasmania, Hobart 7001 Tasmania, Australia*

Complete contact information is available at: https://pubs.acs.org/10.1021/acsomega.2c06228

Notes

The authors declare no competing financial interest.

ACKNOWLEDGMENTS

This work was supported by the Australian Research Council (ARC) via the Centre of Excellence for Electromaterials Science (ACES) (Project CE140100012) and Discovery Project DP170102572, and the Australian National Fabrication Facility (ANFF)-Materials Node. The authors also gratefully acknowledge the assistance of Gregory Ryder and David Officer at the University of Wollongong for providing LCGO. materials.

ABBREVIATIONS

BSA	bovine serum albumin
ITP	isotachophoresis
ssDNA	single-stranded DNA
cDNA	complementary DNA
dsDNA	double-stranded DNA
GO	graphene oxide
LCGO	liquid crystalline graphene oxide

REFERENCES

(1) Sinden, R. R. Introduction to the Structure, Properties, and Reactions of DNA. In *DNA Structure and Function*; 1st ed.; Sinden, R. R., Ed.; Academic Press, 1994; pp 1−57.

(2) Tothill, I. E. Biosensors for cancer markers diagnosis. *Semin. Cell Dev. Biol.* **2009**, *20*, 55−62.

(3) Bokelmann, L.; Nickel, O.; Maricic, T.; Pääbo, S.; Meyer, M.; Borte, S.; Riesenberg, S. Point-of-care bulk testing for SARS-CoV-2 by combining hybridization capture with improved colorimetric LAMP. *Nat. Commun.* **2021**, *12*, No. 1467.

(4) Marras, S. A.; Tyagi, S.; Kramer, F. R. Real-time assays with molecular beacons and other fluorescent nucleic acid hybridization probes. *Clin. Chim. Acta* **2006**, *363*, 48−60.

(5) Goris, J.; Konstantinidis, K. T.; Klappenbach, J. A.; Coenye, T.; Vandamme, P.; Tiedje, J. M. DNA−DNA hybridization values and their relationship to whole-genome sequence similarities. *Int. J. Syst. Evol. Microbiol.* **2007**, *57*, 81−91.

(6) Whitesides, G. M. The origins and the future of microfluidics. *Nature* **2006**, *442*, 368−373.

(7) Sackmann, E. K.; Fulton, A. L.; Beebe, D. J. The present and future role of microfluidics in biomedical research. *Nature* **2014**, *507*, 181−189.

(8) Situma, C.; Hashimoto, M.; Soper, S. A. Merging microfluidics with microarray-based bioassays. *Biomol. Eng.* **2006**, *23*, 213−231.

(9) Weng, X.; Jiang, H.; Li, D. Microfluidic DNA hybridization assays. *Microfluid. Nanofluid.* **2011**, *11*, 367−383.

(10) Zou, F.; Ruan, Q.; Lin, X.; Zhang, M.; Song, Y.; Zhou, L.; Zhu, Z.; Lin, S.; Wang, W.; Yang, C. J. Rapid, real-time chemiluminescent detection of DNA mutation based on digital microfluidics and pyrosequencing. *Biosens. Bioelectron.* **2019**, *126*, 551−557.

(11) Henry, O. Y. F.; O'Sullivan, C. K. Rapid DNA hybridization in microfluidics. *Trac, Trends Anal. Chem.* **2012**, *33*, 9−22.

(12) Salva, M. L.; Rocca, M.; Hu, Y.; Delamarche, E.; Niemeyer, C. M. Complex nucleic acid hybridization reactions inside capillary-driven microfluidic chips. *Small* **2020**, *16*, No. 2005476.

(13) Martins, D.; Wei, X.; Levicky, R.; Song, Y.-A. Integration of multiplexed microfluidic electrokinetic concentrators with a morpholino microarray via reversible surface bonding for enhanced DNA hybridization. *Anal. Chem.* **2016**, *88*, 3539−3547.

(14) Li, X.; Tian, J.; Shen, W. Thread as a versatile material for low-cost microfluidic diagnostics. *ACS Appl. Mater. Interfaces* **2010**, *2*, 1−6.

(15) Tan, W.; Powles, E.; Zhang, L.; Shen, W. Go with the capillary flow. Simple thread-based microfluidics. *Sens. Actuators, B* **2021**, *334*, No. 129670.

(16) Weng, X.; Kang, Y.; Guo, Q.; Peng, B.; Jiang, H. Recent advances in thread-based microfluidics for diagnostic applications. *Biosens. Bioelectron.* **2019**, *132*, 171−185.

(17) Cabot, J. M.; Breadmore, M. C.; Paull, B. Thread based electrofluidic platform for direct metabolite analysis in complex samples. *Anal. Chim. Acta* **2018**, *1000*, 283−292.

(18) Nilghaz, A.; Hoo, S.; Shen, W.; Lu, X.; Chan, P. P. Y. Multilayer cell culture system supported by thread. *Sens. Actuators, B* **2018**, *257*, 650−657.

(19) Agustini, D.; Fedalto, L.; Bergamini, M. F.; Marcolino-Junior, L. H. Microfluidic thread based electroanalytical system for green chromatographic separations. *Lab Chip* **2018**, *18*, 670−678.

(20) Chen, L.; Cabot, J. M.; Paull, B. Thread-based isotachophoresis for DNA extraction and purification from biological samples. *Lab Chip* **2021**, *21*, 2565−2573.

(21) Tomimuro, K.; Tenda, K.; Ni, Y.; Hiruta, Y.; Merkx, M.; Citterio, D. Thread-based bioluminescent sensor for detecting multiple antibodies in a single drop of whole blood. *ACS Sens.* **2020**, *5*, 1786−1794.

(22) Tang, X.; Bansaruntip, S.; Nakayama, N.; Yenilmez, E.; Chang, Y.-l.; Wang, Q. Carbon nanotube DNA sensor and sensing mechanism. *Nano Lett.* **2006**, *6*, 1632−1636.

(23) Loan, P. T. K.; Zhang, W.; Lin, C.-T.; Wei, K.-H.; Li, L.-J.; Chen, C.-H. Graphene/MoS2 heterostructures for ultrasensitive detection of DNA hybridisation. *Adv. Mater.* **2014**, *26*, 4838−4844.

(24) Yang, K.; Feng, L.; Shi, X.; Liu, Z. Nano-graphene in biomedicine: theranostic applications. *Chem. Soc. Rev.* **2013**, *42*, 530−547.

(25) Jeon, J. W.; Cho, S. Y.; Jeong, Y. J.; Shin, D. S.; Kim, N. R.; Yun, Y. S.; Kim, H.-T.; Choi, S. B.; Hong, W. G.; Kim, H. J.; et al. Pyroprotein-based electronic textiles with high stability. *Adv. Mater.* **2017**, *29*, No. 1605479.

(26) Yun, Y. J.; Hong, W. G.; Kim, W.-J.; Jun, Y.; Kim, B. H. A novel method for applying reduced graphene oxide directly to electronic textiles from yarns to fabrics. *Adv. Mater.* **2013**, *25*, 5701−5705.

(27) Liu, B.; Salgado, S.; Maheshwari, V.; Liu, J. DNA adsorbed on graphene and graphene oxide: Fundamental interactions, desorption and applications. *Curr. Opin. Colloid Interface Sci.* **2016**, *26*, 41−49.
(28) Lu, C.-H.; Yang, H.-H.; Zhu, C.-L.; Chen, X.; Chen, G.-N. A graphene platform for sensing biomolecules. *Angew. Chem., Int. Ed.* **2009**, *48*, 4785−4787.
(29) He, S.; Song, B.; Li, D.; Zhu, C.; Qi, W.; Wen, Y.; Wang, L.; Song, S.; Fang, H.; Fan, C. A graphene nanoprobe for rapid, sensitive, and multicolor fluorescent DNA analysis. *Adv. Funct. Mater.* **2010**, *20*, 453−459.
(30) Wu, M.; Kempaiah, R.; Huang, P.-J. J.; Maheshwari, V.; Liu, J. Adsorption and desorption of DNA on graphene oxide studied by fluorescently labeled oligonucleotides. *Langmuir* **2011**, *27*, 2731−2738.
(31) Stine, R.; Robinson, J. T.; Sheehan, P. E.; Tamanaha, C. R. Real-time DNA detection using reduced graphene oxide field effect transistors. *Adv. Mater.* **2010**, *22*, 5297−5300.
(32) Liu, B.; Sun, Z.; Zhang, X.; Liu, J. Mechanisms of DNA sensing on graphene oxide. *Anal. Chem.* **2013**, *85*, 7987−7993.
(33) Dong, H.; Gao, W.; Yan, F.; Ji, H.; Ju, H. Fluorescence resonance energy transfer between quantum dots and graphene oxide for sensing biomolecules. *Anal. Chem.* **2010**, *82*, 5511−5517.
(34) Han, C. M.; Katilius, E.; Santiago, J. G. Increasing hybridization rate and sensitivity of DNA microarrays using isotachophoresis. *Lab Chip* **2014**, *14*, 2958−2967.
(35) Marshall, L. A.; Han, C. M.; Santiago, J. G. Extraction of DNA from malaria-infected erythrocytes using isotachophoresis. *Anal. Chem.* **2011**, *83*, 9715−9718.
(36) Bercovici, M.; Han, C. M.; Liao, J. C.; Santiago, J. G. Rapid hybridization of nucleic acids using isotachophoresis. *Proc. Natl. Acad. Sci.* **2012**, *109*, 11127−11132.
(37) Jeon, S.-H.; Hwang, K.-H.; Lee, J. S.; Boo, J.-H.; Yun, S. H. Plasma treatments of wool fiber surface for microfluidic applications. *Mater. Res. Bull.* **2015**, *69*, 65−70.
(38) Aboutalebi, S. H.; Gudarzi, M. M.; Zheng, Q. B.; Kim, J.-K. Spontaneous formation of liquid crystals in ultralarge graphene oxide dispersions. *Adv. Funct. Mater.* **2011**, *21*, 2978−2988.
(39) Jalili, R.; Aboutalebi, S. H.; Esrafilzadeh, D.; Shepherd, R. L.; Chen, J.; Aminorroaya-Yamini, S.; Konstantinov, K.; Minett, A. I.; Razal, J. M.; Wallace, G. G. Scalable one-step wet-spinning of graphene fibers and yarns from liquid crystalline dispersions of graphene oxide: Towards multifunctional textiles. *Adv. Funct. Mater.* **2013**, *23*, 5345−5354.
(40) Liu, J.; Fu, S.; Yuan, B.; Li, Y.; Deng, Z. Toward a universal "Adhesive Nanosheet" for the assembly of multiple nanoparticles based on a protein-induced reduction/decoration of graphene oxide. *J. Am. Chem. Soc.* **2010**, *132*, 7279−7281.
(41) Chen, L.; Ghiasvand, A.; Sanz Rodriguez, E.; Innis, P. C.; Paull, B. Nanomaterial-assisted thread-based isotachophoresis with on-thread solute trapping. *Analyst* **2022**, *147*, 1944−1951.
(42) Khurana, T. K.; Santiago, J. G. Sample zone dynamics in peak mode isotachophoresis. *Anal. Chem.* **2008**, *80*, 6300−6307.
(43) Min, S. K.; Kim, W. Y.; Cho, Y.; Kim, K. S. Fast DNA sequencing with a graphene-based nanochannel device. *Nat. Nanotechnol.* **2011**, *6*, 162−165.
(44) Liu, J. Adsorption of DNA onto gold nanoparticles and graphene oxide: surface science and applications. *Phys. Chem. Chem. Phys.* **2012**, *14*, 10485−10496.
(45) Zhao, Z.; Li, Q.; Chen, L.; Zhao, Y.; Gong, J.; Li, Z.; Zhang, J. A thread/fabric-based band as a flexible and wearable microfluidic device for sweat sensing and monitoring. *Lab Chip* **2021**, *21*, 916−932.
(46) Terse-Thakoor, T.; Punjiya, M.; Matharu, Z.; Lyu, B.; Ahmad, M.; Giles, G. E.; Owyeung, R.; Alaimo, F.; Shojaei Baghini, M.; Brunyé, T. T.; Sonkusale, S. Thread-based multiplexed sensor patch for real-time sweat monitoring. *npj Flexible Electron.* **2020**, *4*, No. 18.
(47) Mostafalu, P.; Akbari, M.; Alberti, K. A.; Xu, Q.; Khademhosseini, A.; Sonkusale, S. R. A toolkit of thread-based microfluidics, sensors, and electronics for 3D tissue embedding for medical diagnostics. *Microsyst. Nanoeng.* **2016**, *2*, 16039.
(48) Hu, L.; Bian, Z.; Li, H.; Han, S.; Yuan, Y.; Gao, L.; Xu, G. [Ru(bpy)2dppz]2+ electrochemiluminescence switch and its applications for DNA interaction study and label-free ATP aptasensor. *Anal. Chem.* **2009**, *81*, 9807−9811.

https://doi.org/10.1021/acsomega.2c06228
ACS Omega 2023, 8, 13569−13577